# Exploitation of Sentinel-1 SAR data for studying geodynamic, tropospheric and ionospheric processes.

István Bozsó, Eszter Szűcs, László Bányai, Viktor Wesztergom

MTA CSFK Geodetic and Geophysical Institute

2019.02.28.

# Introduction

InSAR technology: Synthetic Aperture Radar (SAR) based interferometry:

- SAR images: ground-based, airplane, UAV, satellite
- high resolution; $20\mathrm{m} \times 5\mathrm{m}$ sized pixels - Low Earth Orbit C-band (5.405 MHz) SAR satellites
- each pixel: amplitude and phase represented as a complex number
- single scene phases are random
- formation of an interferogram (IFG): phase differences between two SAR scenes

# Phase of an interferogram

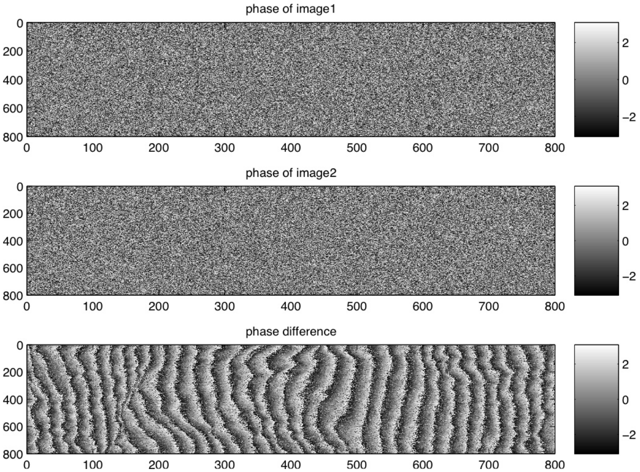


$$\phi\{k,l\} = A_1\{k,l\} e^{i\psi_1\{k,l\}} \times A_2\{k,l\} e^{-i\psi_2\{k,l\}}$$

# Phase of the interferogram

$$\Phi_{\text{IFG}} = \Phi_{\text{defo.}} + \Phi_{\text{atmo.}} + \Phi_{\text{topo.}} + \Phi_{\text{orbit}} + \Phi_{\text{noise}}$$

- $\Phi_{\text{IFG}}$: phase of the interferogram
- $\Phi_{\text{defo.}}$ : phase caused by surface deformation, that occurred between the two SAR acquisitions, in the Line-of-Sight (LOS) direction
- $\Phi_{\text{atmo.}}$: phase caused by the change in atmospheric microwave propagation speed
- $\Phi_{\text{topo.}}$: phase due to topography
- $\Phi_{\text{orbit}}$: phase from errors of the orbital state vector
- $\Phi_{\text{noise}}$: noise from residual phase terms, that cannot be modeled

# Processing the interferometric phase

$$\Phi_{\text{IFG}} = \Phi_{\text{defo.}} + \Phi_{\text{atmo.}} + \Phi_{\text{topo.}} + \Phi_{\text{orbit}} + \Phi_{\text{noise}}$$

Separation and estimation of the different phase terms:

- $\Phi_{\text{topo.}}$: using DEM, residuals correlated with baseline
- $\Phi_{\text{atmo.}}$: atmopsheric models, temporal filtering
- $\Phi_{\text{oribt}}$: more precise orbit data, deramping
- spatial filtering Goldstein-filter[1]

[1] **ZebkerGoldstein1986**.

# Deformation

If estimation of $\Phi_{\text{defo.}}$ is done $\rightarrow$ phase unwrapping $\rightarrow$ LOS deformation.

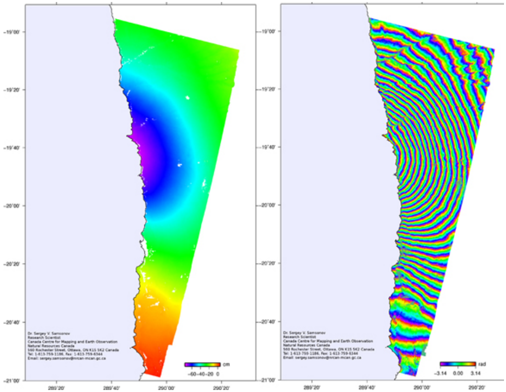


$$d_{\text{defo.}} = \frac{\lambda}{4\pi} \Phi_{\text{defo.,unwrapped}}$$

Multiple interferograms $\rightarrow$ time-series analysis $\rightarrow$ LOS deformation time-series.

# Examples of InSAR applications: Mapping surface displacement based on natural scatterers

# Mapping surface displacement based on natural scatterers

- $\approx$ 3.5 years of Sentinel-1 A descending orbit data (105 scenes)
- covering the Praid salt extrusion in Carpathian Bend area
- salt deformation governed by weather phenomena
- TopoTransyvania project: investigation of the Carpathian Bend and subduction zone
- analyse geodynamic processes (seismic activity, post volcanic activity, salt tectonics)
- SAR images processed with the Gamma Software REF

# Mapping surface displacement based on natural scatterers

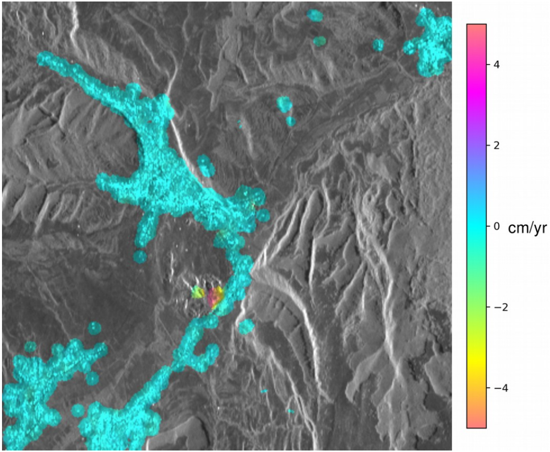


First results show deformation on the southern flanks of the salt diapir. Subsidence is in the $3-4$ cm/yr range. Lack of scatterers on the top of the salt diapir $\rightarrow$ artificial reflectors.

# Mapping surface displacement based on natural scatterers

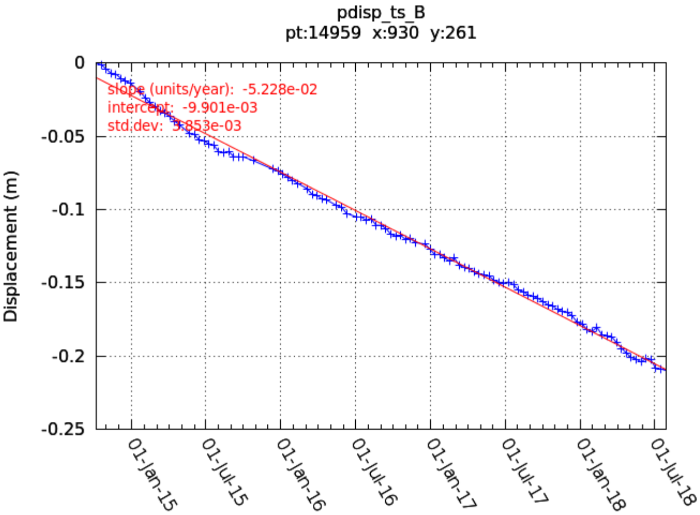


Clear trend of near constant velocity deformation away from the satellite.

# Examples of InSAR applications: Monitoring the displacement time-series of benchmark reflector networks

# Monitoring the displacement time-series of benchmark reflector networks

- $\approx$ 1 year of Sentinel-1 A and B ascending and descending orbit data
- geodetic/geodynamic integrated benchmarks (IBs)
- IB network, settlement (Dunaszekcső) along the loess banks of the Danube
- GNSS measurements 1 year apart
- 3D displacements from combination of InSAR and GNSS data with Kalman filtering
- SAR images processed with Gamma and StaMPS software REF

# Monitoring the displacement time-series of benchmark reflector networks

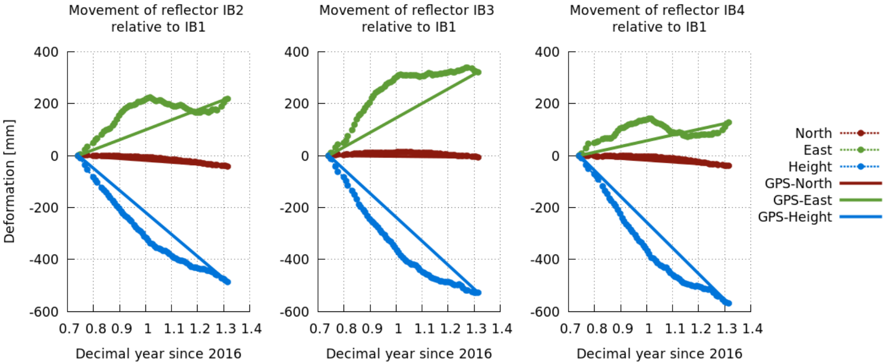


Similar time-series for all 3 moving reflectors, subsidence and movement towards the east (Danube).

# Examples of InSAR applications: Estimation of Integrated Water Vapor (IWV) maps using InSAR

# Estimation of Integrated Water Vapor (IWV) maps using InSAR

- Sentinel-1 A and B ascending dataset covering the area around previously described benchmarks
- assumptions:
  - no surface displacement (except for the landslide area)
  - IFG phase due to change in IWV dominates over IFG phase caused by change in pressure and temperature profiles
- calculation of Zenith Wet Delay (ZWD) changes and converting them into absolute ZWV values using the ECMWF ERA-Interim model
- conversion of ZWD into IWD:

$$\frac{\mathrm{ZWD}}{\mathrm{IWD}} = 10^{-8} \left( k_2 - \frac{R_d}{R_w} k_1 + \frac{k_3}{T_m} \right) R_w$$

$$T_m = 70.2 + 0.72\, T_s$$

Constants: $k_1$, $k_2$, $k_3$, $R_d$, $R_w$ REFS

- SAR images processed with Gamma and StaMPS software REF

# Estimation of Integrated Water Vapor (IWV) maps using InSAR

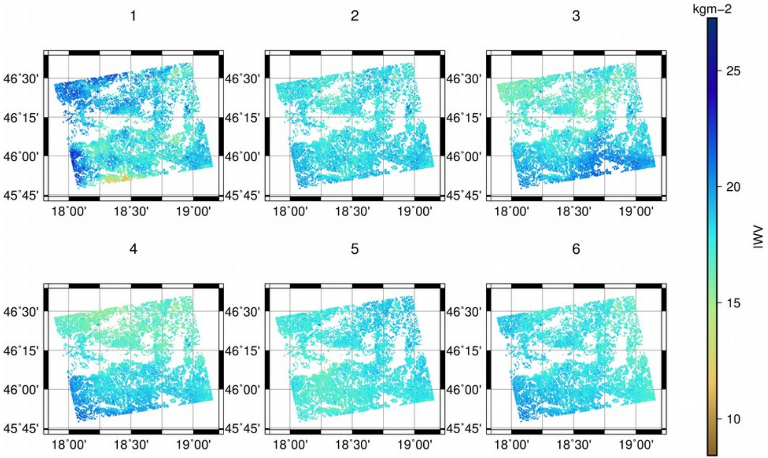


Integrated Water Vapor (IWV) values. Dates: 1 - 2016.09.24., 2 - 2016.10.06., 3 - 2016.10.16., 4 - 2016.10.24., 5 - 2016.12.30., 6 - 2016.12.05.

# Examples of InSAR applications: Calculation of slant range ionospheric TEC differences

# Calculation of slant range ionospheric TEC differences

- two PALSAR-1 SAR scenes covering the Yamagochi Prefecture in Japan, L-band, more sensitive to ionospheric effects
- dispersive propagation of electromagnetic waves in ionosphere, phase delay depends on frequency
- filtering IFG creating high and low sub-band IFGs, $\Delta\mathrm{TEC}$ is proportional to sub-band IFG phase differences REF
- robust method developed by REF based on REF:

$$\Phi_{\text{iono.}} = x\Phi_0 + y(\Phi_{\text{high}} - \Phi_{\text{low}}) = \frac{4\pi K}{c f_0}\Delta\mathrm{TEC}$$

  Constants: $x$, $y$ depend on sub-band frequencies, $K = 40.31\ \mathrm{m}^3\mathrm{s}^{-2}$, $c$ - speed of light, $f_0$ - radar center frequency
- SAR images processed with Gamma and StaMPS software REF

# Calculation of slant range ionospheric TEC differences

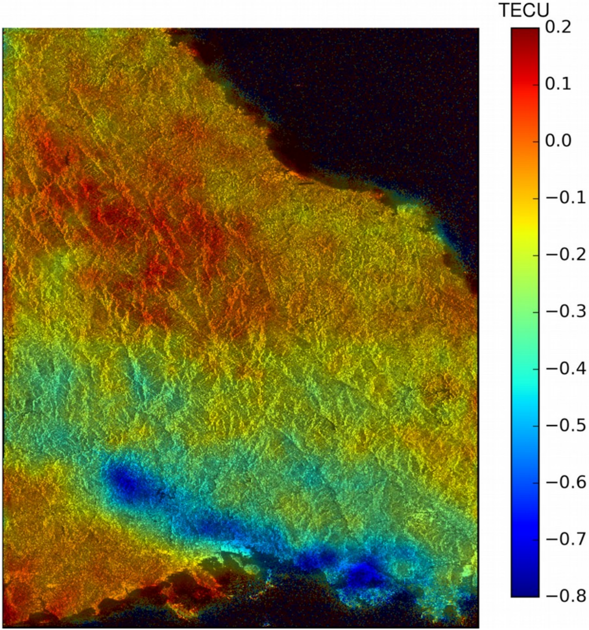


Total Electron Content (TEC) changes between 2009.03.28. and 2009.06.28. above the Yamagochi Prefecture Japan. TEC changes are relative to the upper left corner of the SAR scene. 1 TECU $= 10^{16}\ \mathrm{electron}/\mathrm{m}^2$. Background image is the SAR backscatter intensity image of the 2009.03.28. scene.

## Discussion

- multiple applications of InSAR technology
- Sentinel-1 extremely useful for monitoring surface deformation
- estimation of slant-range and vertical integrated quantities (IWV, TEC) describing the state of the atmosphere
- long-term time series of integrated quantities: trends, their correlation, troposphere - ionosphere interaction

## Future plans

- Refinement of deformation monitoring techniques.
- $\Delta \mathrm{TEC}$ estimation based on Sentinel-1 images
- IWV calculation without the need for auxiliary data (weather model).

# Thank you for your attention!

## Acknowledgement

Contains modified Copernicus Sentinel data 2014-2018, processed by ESA.

This study was supported by the TopoTransylvania - a multidisciplinary Earth science initiative in Central Europe to tackle local and global challenges project (NKFI NN 128629).